

# Theta Rhythm Selection in the Dentate Gyrus: Experiments and Simulation

Katsumi Tateno<sup>†</sup>, Satoru Ishizuka<sup>†</sup>, Kohshi Nakashima<sup>‡</sup> and Hatsuo Hayashi<sup>†</sup>

<sup>†</sup>Department of Brain Science and Engineering, Kyushu Institute of Technology  
2-4 Hibikino, Wakamatsu-ku, Kitakyushu 808-0196 Japan

<sup>‡</sup>Information Science Center, Kyushu Institute of Technology  
1-1 Sensui-cho, Tobata-ku, Kitakyushu 804-8550 Japan

Email: tateno@brain.kyutech.ac.jp, ishizuka@brain.kyutech.ac.jp, naka@isc.kyutech.ac.jp, hayashi@brain.kyutech.ac.jp

**Abstract**—Spread of epileptic activity of the entorhinal cortex is prevented by the hippocampal dentate gyrus. On the other hand, granule cells in the dentate gyrus well fire during theta rhythm. The dentate gyrus may work as a band-pass filter for the theta rhythm. We here present properties of theta rhythm selection in the dentate gyrus in rat hippocampal slices and propose a computational dentate gyrus model that accounts for the rhythm selection.

## 1. Introduction

Granule cells in the hippocampal dentate gyrus are deeply hyperpolarized in slice preparations. The dentate gyrus prevents spread of epileptiform activity from the entorhinal cortex [1][2][3]. On the other hand, in *in vivo* experiment, during theta rhythm, the granule cells show repetitive firing. Firings of granule cells are phased locked with the theta rhythm. Muñoz *et al.* have suggested that the dentate gyrus works as theta rhythm selection [4]. It seems that the dentate gyrus preferably transmit theta rhythm to the hippocampal CA3 region. However, the theta rhythm selection has not been confirmed in the hippocampal slice preparations. In the present study, we show properties of the theta rhythm selection using horizontal slices of the dentate gyrus.

Hilar region is located between the dentate gyrus and the hippocampal CA3 region. Mossy cells in the hilar region frequently receive excitatory synaptic input from granule cells and CA3 pyramidal cells [5][6]. The mossy cells connect granule cells and interneurons in the dentate gyrus [7]. Feedback loops including the mossy cells can contribute to filtering properties of the dentate gyrus.

We have shown filtering properties of a fundamental dentate gyrus network model [8]. Random synaptic input to mossy cells leads to properties of a band-pass filter in the fundamental dentate gyrus network model. The properties of a band-pass filter depend on a variance of the random synaptic input to the mossy cells. In the present study, we propose a larger-scaled dentate gyrus network model. In the fundamental network model, we assumed a source of random synaptic input to mossy cells. In fact, granule cells and CA3 pyramidal cells are sources of the random synaptic input to the mossy cells. Here we prepare several granule cells as presynaptic neurons for mossy cells.

The entorhinal cortex shows synchronized activity of neural population that is sent to the dentate gyrus. Theta rhythm is also a partially synchronized activity. We believe that synchronized activity may contribute to signal processing in the hippocampus. In the present study, we suggest a possible contribution of synchronized neural activity to filtering properties. The periodic synaptic input and the random synaptic input were delivered to the dentate gyrus network model. Filtering properties of the dentate gyrus network model depend on the degree of synchronization of granule cells.

## 2. Methods

### 2.1. Experimental Procedure

We prepared 400  $\mu\text{m}$  thick horizontal hippocampal slices from male Wistar rats, 3-5 weeks of age (60-130 g) (Fig.1). The dentate gyrus was separated from CA1 and CA3 regions by a sharp knife. This isolation prevents interactions between the dentate gyrus and CA1/CA3. The hippocampal slices were placed on the liquid/gas interface chamber maintained at  $34 \pm 0.5$  °C. Artificial cerebrospinal fluid was bubbled with 95% O<sub>2</sub> and 5% CO<sub>2</sub>. Field potential was recorded by a glass microelectrode (tip diameter: 20-30  $\mu\text{m}$ ). The recording electrode was placed at the granule cell layer in the dentate gyrus. The perforant path was stimulated by a fine bipolar electrode.

Periodic 20 current pulses were delivered to the perforant path. The range of the input frequency was 0.1 to 100 Hz. Field potentials to the perforant path stimulation were recorded. We averaged the amplitude of the population spikes.

### 2.2. Dentate Gyrus Network Model

We proposed a fundamental network model of the dentate gyrus [8]. The fundamental network model consists of 2 granule cells, 2 basket cells, and 2 mossy cells. The granule cells connected the basket cells through excitatory synapses. The basket cells inhibited the granule cells. The granule cells also connected the mossy cells through excitatory synapses. The mossy cells connected the granule cells and the basket cell through excitatory synapses. The mossy

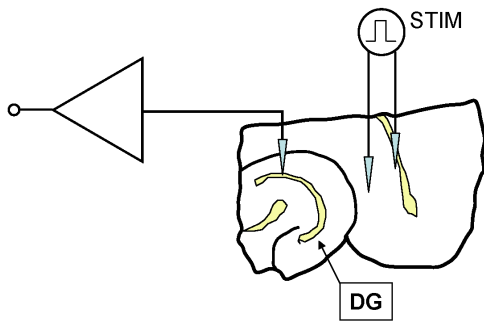


Figure 1: Slice preparation of the hippocampal dentate gyrus. The electrical stimulation was delivered to the perforant path fibers (STIM).

cells received excitatory synaptic input from sources of random signals. Inter-pulse intervals of the random synaptic input to the mossy cells were drawn from a negative exponential distribution. The mean interval was 30 ms. We varied the standard deviation of the exponential distribution between 0 and 30 ms.

The fundamental network model can be extended to a larger-scaled network model. We assumed an exponential distribution as a source of random synaptic input to mossy cells in the fundamental network model. As mossy cells, in fact, receive synaptic input from granule cells and CA3 pyramidal cells, the source of random synaptic input to mossy cells can be replaced by population activity of granule cells. In the present dentate gyrus network model, the mossy cells receive excitatory synaptic input from the granule cells. The granule cells receive random synaptic input by the perforant path stimulation. The dentate gyrus network model proposed here consists of 9 granule cells, 9 basket cells, and 3 mossy cells. The network structure is shown in Fig. 2. A granule cell innervates a basket cell and 3 mossy cells. The basket cells give inhibitory synaptic input to the granule cells. This is a feedback inhibition to the granule cells. Each mossy cell gives excitatory synaptic input to 6 granule cells and 6 basket cells. The mossy cells give lateral inhibition to the granule cells through the basket cells. Refer to Appendix for equations of each neuron model.

### 2.3. Frequency Characteristics

We delivered 100 periodic pulses to  $N_{\text{sync}}$  granule cells and  $N_{\text{sync}}$  basket cells through synapses.  $N_{\text{sync}}$  is the number of common perforant path fibers to both types of cell. The number of spikes of the granule cell #1 was counted. The firing probability was defined as the ratio of the number of spikes to the number of the periodic pulses. Random synaptic input was also delivered to the granule cells ( $9 - N_{\text{sync}}$ ). Here  $N_{\text{sync}}$  was 3, 6, or 9.

The mean interval of the random synaptic input to gran-

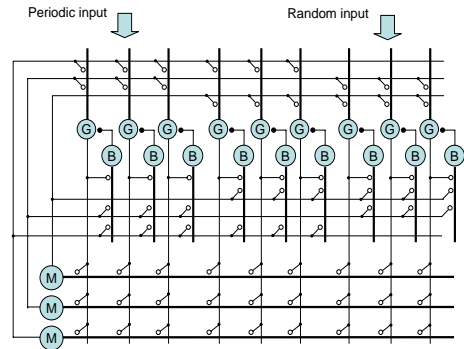


Figure 2: The dentate gyrus network model. Periodic synaptic input and random synaptic input were delivered to the granule cells and the basket cells through the perforant path.

ule cells was 50 ms. The standard deviation of the random synaptic input was 25 ms. The inter-pulse interval of the random synaptic input was drawn from an exponential distribution. The synaptic weight for the random synaptic input was  $0.06 \mu\text{S}$ .

## 3. Results

### 3.1. Theta Rhythm Selection at the Dentate Gyrus in Hippocampal Slice Preparations

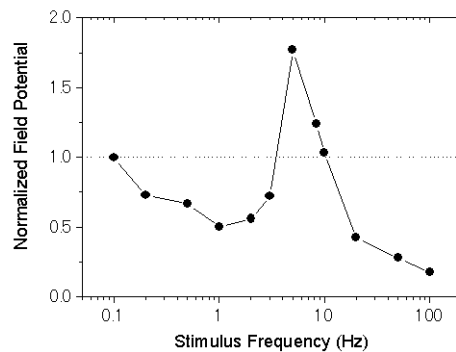


Figure 3: Filtering properties of the dentate gyrus in hippocampal slice preparations.

The perforant path stimulation evoked population spikes at the granule cell layer in the hippocampal dentate gyrus. Figure 3 shows the mean amplitude of the population spikes evoked by the periodic perforant path stimulation. The amplitude of the population spikes were normalized by the amplitude at 0.1 Hz. The amplitude of the population spike depended on the input frequency of the perforant path stimulation. At 5 Hz, the population spike was about 1.8 times as large as the population spike at 0.1 Hz. Hippocampal slice preparations vary in the stimulus frequency that causes the maximum amplitude from 5 to 10 Hz. The

frequency range of 5 - 10 Hz corresponds to the frequency range of theta rhythm. The amplitude of the population spike decreased in the frequency range above 5 Hz. Furthermore, application of the GABA<sub>A</sub> receptor antagonist, bicuculline, removed properties of the theta rhythm selection. Bicuculline enhanced the amplitude of the population spike in the higher frequency range (20 - 100 Hz). However, the size of the population spike in the frequency range between 0.2 - 1 Hz was not changed by bicuculline.

### 3.2. Rhythm Selection in a Dentate Gyrus Network Model

We first introduce filtering properties of our fundamental dentate gyrus network model. In the frequency range between 2 - 5 Hz, the firing probability was larger than 90 %. The firing probability at 5 Hz was about 2.5 times as large as the firing probability at 0.2 Hz. The higher frequency input reduced the firing probability. Without the random synaptic input to the mossy cells, the dentate gyrus network model showed properties of a low-pass filter.

Degree of synchronization in the perforant path input modified filtering properties of the present dentate gyrus network model. In the present study, the number of synchronized periodic synaptic input was varied. The firing probability depended on the number of synchronized periodic input  $N_{sync}$ . When  $N_{sync} = 3$ , the firing probability was generally suppressed in the whole input frequency range. At  $N_{sync} = 6$ , the frequency characteristics of the firing probability were likely to be a band-pass filter (Fig.4). The firing probability was almost 100% in the input frequency range of 3 - 5 Hz, while less 70 % at 0.5 Hz. As the firing probability was improved in the low frequency range, a large  $N_{sync}$  (=9) caused properties of a low-pass filter.

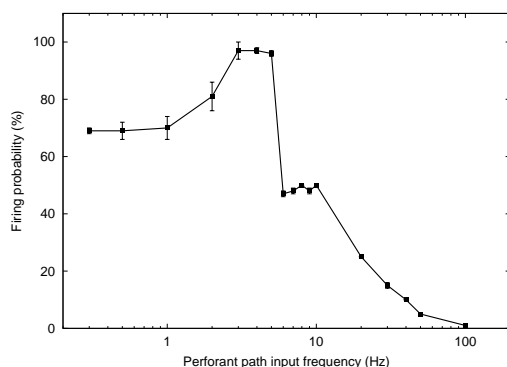


Figure 4: Firing probability as a function of the perforant path input frequency in the dentate gyrus network model.  $N_{sync} = 6$ .

## 4. Discussion

The hippocampal dentate gyrus well responded to the stimulus frequency ranging between 5 - 10 Hz in the ex-

periment. The stimulus frequency range between 5 - 10 Hz corresponds to the frequency range of theta rhythm. The stimulus frequency that caused maximum response depended on the preparation. The amplitude of fEPSP did not depend on the stimulus frequency (data not shown). This indicates that internal synaptic connections in the dentate gyrus contribute to the theta rhythm selection.

The properties of a band-pass filter are caused by random synaptic input to mossy cells in the present dentate gyrus network model. Synaptic projection from granule cells causes the random synaptic input to mossy cells. Probability distribution of the random synaptic input to mossy cells is determined by the degree of synchronization in population activity of granule cells. A suitable degree of synchronization in population activity of granule cells can lead to the properties of a band-pass filter. In the periodic perforant path input frequency range below 2 Hz, the mossy cells stochastically fire by random synaptic input through the granule cells. Random firing of the mossy cells prevents the periodic perforant path input. In the periodic perforant path input frequency range between 3 - 5 Hz, as the mossy cells are phase-locked with the periodic perforant path input, the periodic perforant path input is not prevented. In the frequency range of 6 Hz or higher, the feedback and the feed-forward inhibitions through the basket cells prevent firing of the granule cells. Well synchronized periodic perforant path input does not generate the random synaptic input to the mossy cells. This causes properties of a low-pass filter in the dentate gyrus network model. Poor synchronization in the granule cells input is buried under the random perforant path input. The random perforant path input inhibits most periodic perforant path input. Those results indicate that the degree of synchronization in neural population activity can contribute to modifying filtering properties in the dentate gyrus network model.

## Acknowledgments

This work has been supported by the Ministry of Education, Culture, Sports, Science and Technology (the 21<sup>st</sup> Century Center of Excellence Program in Kyushu Institute of Technology, entitled "World of brain computing interwoven out of animals and robots", and Grant-in-Aid for Scientific Research No.16015289)

## References

- [1] J. Behr, K. J. Lyson and I. Mody, "Enhanced propagation of epileptiform activity through the kindled dentate gyrus," *J. Neurophysiol.*, vol.79, pp.1726-1732, 1998.
- [2] R. C. Collins, R. G. Tearse and E. W. Lothman, "Functional anatomy of limbic seizures: focal discharges from medial entorhinal cortex in rat," *Brain Res.*, vol.280, pp.25-40, 1983.

- [3] U. Heinemann, H. Beck, J. P. Dreier, E. Ficker, J. Stabel and C. L. Zhang, "The dentate gyrus as a regulated gate for the propagation of epileptiform activity," *Epilepsy Res. Suppl.*, vol.7, pp.273–280, 1992.
- [4] M. D. Muñoz, A. Núñez and E. García-Austt, "Frequency potentiation in granule cells *in vivo* at theta frequency perforant path stimulation," *Exp. Neurol.*, vol.113, pp.74–78, 1991.
- [5] H. E. Scharfman, D. D. Kunkel and P. A. Schwartzkroin, "Synaptic connections of dentate granule cells and hilar neurons: Results of paired intracellular recordings and intracellular horseradish peroxidase injections," *Neurosci.*, vol.37, pp.693–707, 1990.
- [6] H. E. Scharfman, "Evidence from simultaneous intracellular recordings in rat hippocampal slices that area CA3 pyramidal cells innervate dentate hilar mossy cells," *J. Neurophysiol.*, vol.72, pp.2167–2180, 1994.
- [7] H. E. Scharfman, "Electrophysiological evidence that dentate hilar mossy cells are excitatory and innervate both granule cells and interneurons," *J. Neurophysiol.*, vol.74, pp.179–194, 1995.
- [8] K. Tateno, T. Hashimoto, S. Ishizuka, K. Nakashima and H. Hayashi, "Theta rhythm selection of a dentate gyrus network model," *Proceedings of IJCNN 2004*, pp.1529–1532, 2004.
- [9] G. L. F. Yuen and D. Durand, "Reconstruction of hippocampal granule cell electrophysiology by computer simulation," *Neurosci.*, vol.41, pp.411–423, 1991.
- [10] R. D. Traub, R. Miles and G. Buzsáki, "Computer simulation of carbachol-driven rhythmic population oscillations in the CA3 region of the *in vitro* rat hippocampus," *J. Physiol.*, vol.451, pp.653–672, 1992.
- [11] S. Jinno, S. Ishizuka and T. Kosaka, "Ionic currents underlying rhythmic bursting of ventral mossy cells in the developing mouse dentate gyrus," *Eur. J. Neurosci.*, vol.17, pp.1338–1354, 2003.
- [12] P. F. Pinsky and J. Rinzel, "Intrinsic and network rhythmogenesis in a reduced Traub model for CA3 neurons," *J. Comput. Neurosci.*, vol.1, pp. 39–60, 1994.

## Appendix

*Granule cell model* The granule cell model that consists of one somatic and 12 dendritic compartments is based on Yuen and Durand's model [9]. The somatic compartment is given by below:

$$C_m \frac{dV}{dt} = \bar{g}_{Na} m^3 h (E_{Na} - V) + \bar{g}_K n^4 (E_K - V) + \bar{g}_{Ca} e^2 (E_{Ca} - V) + \bar{g}_{K-AHP} q^2 (E_K - V) + g_{Ls} (E_L - V) \quad (1)$$

$$\frac{d[Ca^{2+}]_i}{dt} = -\frac{[Ca^{2+}]_i - [Ca^{2+}]_{i0}}{\tau} - \frac{I_{Ca}}{w \cdot z \cdot F} \quad (2)$$

where  $\tau$  is the  $Ca^{2+}$  removal rate ( $\tau = 9ms$ ),  $w$  is a  $Ca^{2+}$  shell thickness ( $w = 0.2 \mu m$ ),  $z$  is the valence of  $Ca^{2+}$ ,  $F$  is the Faraday constant.  $[Ca^{2+}]_{i0} = 0.1 \mu M$ . The maximal conductances are  $\bar{g}_{Na} = 250 mS/cm^2$ ,  $\bar{g}_K = 40 mS/cm^2$ ,  $\bar{g}_{Ca} = 1 mS/cm^2$ ,  $\bar{g}_{K-AHP} = 4.7 mS/cm^2$ , and  $g_{Ls} = 0.025 mS/cm^2$ . The dendritic compartment has only a passive channel. For the dendritic leakage current,  $g_{Ld} = 0.04 mS/cm^2$ .  $E_{Na} = 45 mV$ .  $E_K = -85 mV$ .  $E_{Ca} = 70 mV$ .  $E_L = -67.46 mV$ .

*Basket cell model* A basket cell model refers to the Traub's model [10]. The basket cell model consists of one somatic and 18 dendritic compartments. The somatic compartment has the fast  $Na^+$  and delayed rectifier  $K^+$  channels. The dendritic compartment has only the leakage current. The basket cell model is a silent neuron that shows a fast and a non-adaptive firing due to depolarizing dc pulse stimulation.

*Mossy cell model* The present mossy cell model consists of one somatic compartment and one dendritic compartment. Fast  $Na^+$  channel (Na), fast delayed rectifier  $K^+$  channel (K), and hyperpolarization-activated channel ( $h$ ) [11] are included in the somatic compartment.  $Ca^{2+}$  channel (Ca),  $Ca^{2+}$ -dependent  $K^+$  channel (K-AHP), and voltage- and  $Ca^{2+}$ -dependent  $K^+$  channel (K-C) are included in the dendritic compartment. The mossy cell model is based on the hippocampal CA3 pyramidal cell model introduced by Pinsky and Rinzel [12]. We adjusted rate functions of the CA3 pyramidal cell to replicate mossy cell specific properties.

$$C_m \frac{dV_s}{dt} = \bar{g}_{Na} m^2 h (E_{Na} - V_s) + \bar{g}_K n (E_K - V_s) + \bar{g}_h a (E_h - V_s) + g_{Ls} (E_L - V_s) \quad (3)$$

$$C_m \frac{dV_d}{dt} = \bar{g}_{Ca} s^2 (E_{Ca} - V_d) + \bar{g}_{K-C} \cdot c \cdot \min(0.004 \cdot [Ca^{2+}]_i, 0.01) \cdot (E_K - V_d) + \bar{g}_{K-AHP} q (E_K - V_d) + g_{Ld} (E_L - V_d) \quad (4)$$

$$\frac{d[Ca^{2+}]_i}{dt} = -0.075 \cdot [Ca^{2+}]_i - 130 \cdot I_{Ca} \quad (5)$$

where  $V_s$  is the somatic membrane potential, and  $V_d$  is the dendritic membrane potential. A unit of  $I_{Ca}$  is  $mA/cm^2$ . The maximal conductances are  $\bar{g}_{Na} = 30 mS/cm^2$ ,  $\bar{g}_K = 15 mS/cm^2$ ,  $\bar{g}_h = 0.22 mS/cm^2$ ,  $\bar{g}_{Ca} = 7 mS/cm^2$ ,  $\bar{g}_{K-C} = 15 mS/cm^2$ ,  $\bar{g}_{K-AHP} = 1 mS/cm^2$ ,  $g_{Ls} = 0.1 mS/cm^2$ , and  $g_{Ld} = 0.1 mS/cm^2$ .  $E_{Na} = 60 mV$ .  $E_K = -75 mV$ .  $E_{Ca} = 80 mV$ .  $E_h = -38 mV$ .  $E_L = -60 mV$ . Electric parameters are as follows: unit membrane resistivity  $R_m = 10000 \Omega \cdot cm^2$ , internal resistivity  $R_i = 681 \Omega \cdot cm$ , and membrane capacitance  $C_m = 3 \mu F/cm^2$ . The somatic area is  $1024 \mu m^2$ . The dendritic area is  $2390 \mu m^2$ .